Application of Cobalt Hexacyanoferrate Coated Fe_3O_4 Nanoparticle for Cesium ion (Cs+) Adsorption

Le Thi Ha Lan, Nguyen Thi Minh Sang, Nguyen Dinh Trung, Nguyen An Son*, Suk Soo Dong
Dalat University, Lam Dong, Viet Nam
Corresponding author: sonna@dlu.edu.vn

1. Introduction

The development of the nuclear industry has produced a lot of long half-life radioactive wastes. Cesium radioactive isotope (^{137}Cs) is the main radioactive material derived from nuclear accident and nuclear waste, accounting for 6.3% of the fission product.

Previous works have demonstrated zeolite [1], ammonium molybdophosphate (AMP), silicotitanate (CST) [2], and ferrocyanide complexes [3] as good cesium absorbent. In particular, ferrocyanide - transition metal complexes (FTMC) have been known as high selective absorbent for cesium [4]. Dwivedi et al. [5] used a micro gel composed of Cobalt hexacyanoferate attached to Alginate to separate cesium from water.

FTMC are selective for cesium, but its the recovery and reusability of ferrocyanide-transition metal complexes are practically difficult due to the dispersion of the particles in the solution. The deposition of FTMC on different substrates is a promising method to solve this problem.

In this paper, the process of synthesis nanocomposite comprising cobalt hexacyanoferate deposited on the surface of Fe_3O_4 nanoparticles is reported. The obtained nanocomposite is applied as cesium absorbent, and its adsorption capacity and mechanism are discussed.

2. Experimental

2.1. Materials

In this study, standard solutions (Cs^+ (1000 mg/L), CsCl, $K_4[Fe(CN)_6$, $CoCl_2.6H_2O$) of 99.99% purity (Merck) were mainly used, and also used are $FeCl_3 \cdot 6H_2O$, $FeCl_2 \cdot 4H_2O$, 25% NH_4OH solution, HNO_3 (0.01-0.1N), NaOH (0.01-0.1 N), and NH_4OH, among others.

2.2. Synthesis of Iron oxide nanoparticles (Fe_3O_4)

An aqueous solution containing $FeCl_3.6H_2O$ and $FeCl_2.4H_2O$ with a molar ratio of 2:1 (filter out the solution if it precipitated) was added into a flask, bubbled by N_2 for 10 min, and heated up to 70^0C in a ultra- sonifier. The above solution was dropwisely added to 25 mL of NH_4OH (25%). The temperature of the chemical reaction was maintained at 70^0C with stirring speed of 1200 rpm. The reaction solution became dark green. After the products were separated by a magnet machine and rinsed several times by distilled water until neutral pH was obtained reaction completion.

2.3. Synthesis of $Co_2[Fe(CN)_6]/Fe_3O_4$

4g of as-prepared Fe_3O_4 nanoparticles were dispersed in 500 ml of $CoCl_2$ solution (0.01 M), which was dropwisely added by 250 mL of $K_4[Fe(CN)_6]$ solution (0.1 M). The temperature of the reaction was maintained at 25^0C and stirring speed of 1200 rpm was applied. After reaction, the dark brown product was separated from the reaction solution by a magnet machine, rinsed with distilled water, and dried at 60^0C.

2.4. Analyses of synthetic materials

The powder X-ray diffraction (PXRD) pattern of materials was collected using a Scintag - XDS-2000 diffractometer with Copper (Cu) K_α (λ = 1.54059 Å) and two-theta (2θ) range from 10^0 to 70^0. Transmission electron microscopy (TEM) images were obtained using JEOL JEM-1400 TEM. The elements in the materials were determined by total reflection X-ray fluorescence spectroscopy analysis (TXRF).

2.5. Determination of cesium adsorption capacity of $Co_2[Fe(CN)_6]/Fe_3O_4$

0.1 g of $Co_2[Fe(CN)_6]/Fe_3O_4$ was added into 100 ml of vary concentrations (from 30 to 90 mg/L) of Cs^+ solution, which was stored in the closed jar, and was shaken at 180 rpm for 24 hours until reached equilibrium absorption at 25^0C. After the adsorption, the material was separated by a magnet machine. The supernatant was centrifuged at 10,000 rpm in 5 min, then filtered through a 0.24 μm filter.

The pH of the solution (3.0, 4.0, 5.0, 6.0, 7.0, 8.0, and 9.0) was adjusted by using HNO_3 (0.01-0.1M) or NaOH (0.01-0.1M). After 24 hours of reaction, the absorbent material was separated by a magnet. The supernatant was centrifuged, filtered, and detected by TXRF.

2.6. Investigation on the reaction rate

0.1 g of $Co_2[Fe(CN)_6]/Fe_3O_4$ was added into 100 ml of a Cs+ solution (0.1 mg/L) which were stored in the jar. This component was shaken at 180 rpm at 25°C in 5 min, and was then taken out in an interval of one minute.

The absorbed cesium content was based on the original and residual concentration of cesium in the solution with following formula:

$$q = \frac{V(C_i - C_e)}{B} \quad (1)$$

where q is the amount of cesium absorbed, or the absorbed capacity of the material (mg/g absorbent); C_i and C_e are Cs^+ concentrations before and after absorption, respectively; V is the volume of solution, and B is the mass of absorbent used.

Langmuir adsorption isotherm equation is given by:

$$q_e = \frac{q_m b C_e}{1 + b C_e} \quad (2)$$

where q_e is the amount of Cs^+ absorbed by the material (mg/g absorbent), q_m is the maximum absorption capacity (MAC) of the Cs^+, C_e is the initial concentration of the adsorption at time, b is the constant of the adsorption/desorption ratio.

Freundlich adsorption isotherm equation is given by:

$$q_e = K C_e^{1/n} \quad (3)$$

where q_e is the amount of Cs^+ absorbed by the material (mg/g); K, n are the adsorption constants when the reaction reaches equilibrium.

All samples of the absorbent material after adsorption experiments were washed several times by distilled water, dried at 60^0C, and then detected by TXRF method. The Cs^+ concentration change in the solution can reveal the adsorption mechanism.

3. Results and discussion

The characterizations of materials were determined by PXRD and TEM. PXRD patterns of Fe_3O_4, $Co_2[Fe(CN)_6]$, and $Co_2[Fe(CN)_6]/Fe_3O_4$ are shown in Fig. 1.

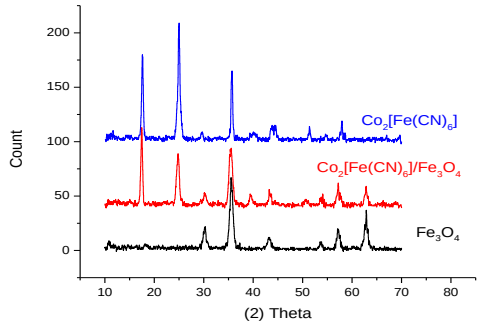

Fig. 1. PXRD patterns of Fe_3O_4, $Co_2[Fe(CN)_6]/Fe_3O_4$, and $Co_2[Fe(CN)_6]$

The PXRD pattern of $Co_2[Fe(CN)_6]/Fe_3O_4$ is clearly composed of both crystalline phases, illustrated by $Co_2[Fe(CN)_6]$ (2θ = 18, 25, 37, 41, and 44^0) and Fe_3O_4(2θ = 65^0), which confirm the successful formation of the composite materials.

Determination of Fe_3O_4 and $Co_2[Fe(CN)_6]/Fe_3O_4$ by TXRF confirms that $Co_2[Fe(CN)_6]/Fe_3O_4$ is composed of several Fe_3O_4 nanoparticles. The molecular weight of $Co_2[Fe(CN)_6]$ is 329.8158 g/mol, and the elemental composition is shown in Table 1.

Table 1. Theoretical element composition of $Co_2[Fe(CN)_6]$

Elements	Molecular weigh	Stoichiometry	Weight percent (%)
Co	58.93	2	35.73
Fe	55.84	1	16.93
C	12.01	6	21.84
N	14.01	6	25.48

According to the theory, the atomic weight ratio of Co/Fe in $Co_2[Fe(CN)_6]/Fe_3O_4$ is ~117/55. From the elemental analysis of $Co_2[Fe(CN)_6]/Fe_3O_4$, the atomic weigh ratio of Co/Fe is ~714/1977. Comparison between theoretical and empirical results shows that the weight percentage of $Co_2[Fe(CN)_6]$ accounts for 20.65% of $Co_2[Fe(CN)_6]/Fe_3O_4$ when $Co_2[Fe(CN)_6]$ is deposited on Fe_3O_4 nanoparticle.

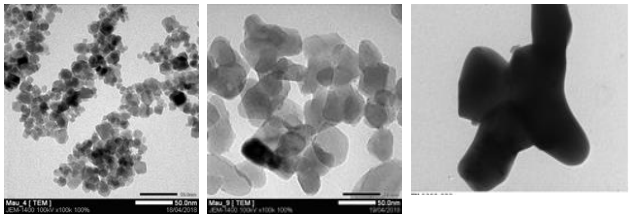

(a) (b) (c)

Fig. 2. TEM images of (a) Fe_3O_4; (b) $Co_2[Fe(CN)_6]/Fe_3O_4$; (c) a high-magnification TEM image of $Co_2[Fe(CN)_6]/Fe_3O_4$

Based on the TEM image in Fig. 2, the increase in particle size upon the deposition of $Co_2[Fe(CN)_6]$ onto Fe_3O_4 nanoparticles is attributed to the aggregate of several Fe_3O_4 nanopartilces, and $Co_2[Fe(CN)_6]$ plays a role as an outer covering layer. The $Co_2[Fe(CN)_6]/Fe_3O_4$ nano composite with the mean size of around 50 nm is used for further Cs^+ absorption studies.

The adsorption happened at 25^0C and pH = 5.0, the results of the Cs^+ absorbent on the materials are shown in Table 2. When the reaction reached the balance condition, the amount of Cs^+ absorbed in the solution was calculated by the formulas (1, 2, 3). The results showed that the process of the balance condition depended on the concentration of the original solution.

Table 2. The absorbed capacity of Cs^+ by $Co_2[Fe(CN)_6]/Fe_3O_4$

(1)	(2)	(3)	(4)	(5)	(6)
30	46.52	0.35	65	52.10	0.39
35	48.11	0.36	70	52.90	0.40
40	49.04	0.37	75	53.30	0.40
45	50.11	0.37	80	53.43	0.40
50	50.24	0.38	85	53.29	0.40
55	51.70	0.39	90	53.37	0.40
60	51.57	0.39			

(1): Cs+ concentration (mg/g)
(2): The absorbed capacity of Cs+ material (mg/g)
(3): The absorbed mili-equivalent of Cs+ material (meq/g)
(4): Cs+ concentration
(5): The absorbed capacity of Cs+ material (mg/g)
(6): The absorbed mili-equivalent of Cs+ material (meq/g)

The experimental results in table 2 shows the appropriation with the Langmuir and Freundlich adsorption isotherm models. Table 3 and Fig. 3 show the parameters of the isothermal adsorption of Cs^+ on $Co_2[Fe(CN)_6]/Fe_3O_4$ which are based on Langmuir and Freundlich adsorption isotherm models. MAC of materials based on Langmuir adsorption isotherm model was q_m = 58.18 mg/g, R^2 = 0.97, and b = 0.13.

Table 3. The parameters of the Langmuir and Freundlich adsorption isotherm models for Cs^+ on $Co_2[Fe(CN)_6]/Fe_3O_4$ adsorption

$Co_2[Fe(CN)_6]/Fe_3O_4$ adsorption			
The Langmuir adsorption isotherm model			
Ion adsorption	qm (mg/g)	b	R^2
Cs^+	58.18	0.13	0.97
The Freundlich adsorption isotherm model			
Ion adsorption	K (L/mg)	1/n	R^2
Cs^+	9.88	0.12	0.95

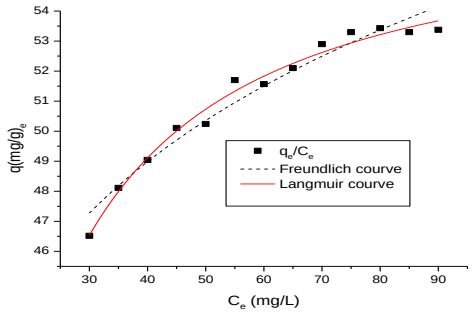

Fig. 3. Cs^+ adsorption isotherm by $Co_2[Fe(CN)_6]/Fe_3O_4$

TXRF method was used for the analysis of $Co_2[Fe(CN)_6]/Fe_3O_4$ sample which adsorbed Cs^+. MAC reached 53.42 mg/g. MAC based on the Langmuir adsorption isotherm model is q_{max} = 58.18 mg/g, that is 4 units higher than the practical value (q_{exp} = 53.42 mg/g). The results show that Co^{2+} after adsorption decreased more than the original sample, and the reaction happened on the surface of $Co_2[Fe(CN)_6]/Fe_3O_4$.

It can be seen in the Fig. 4 (a) that the adsorption process of Cs^+ reached MAC in range pH of 4.0 -5.0; at pH = 4.0, MAC of $Co_2[Fe(CN)_6]/Fe_3O_4$ is 53.67mg/g. At pH = 3.0, MAC of material was low because the surface of absorbent was dissolved. At pH>5, the adsorption process decreased because the surface of absorbent was hydrated to create a film on the surface that limited the contact of Cs^+ absorbent. At pH=4.0, Cs^+ concentration was used in dilute solution during the investigation of reaction rate.

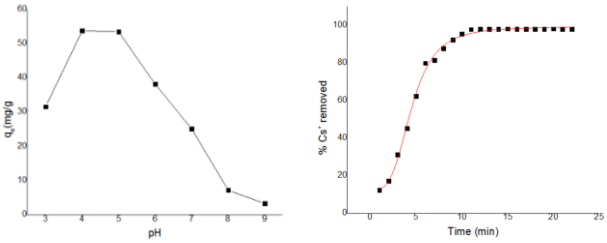

(a) The effective of the absorption capacity on pH (b) Percentage remove of Cs+ depend on time

Fig. 4. The effective of pH and time on the absorption capacity of Cs^+ on $Co_2[Fe(CN)_6]/Fe_3O_4$

It can be seen from the Fig. 4 (b) result that the reaction reached the balance condition in 10 min, and Cs+ is eliminated from the solution up to 98%.

3.3. Mechanism of Cs^+ adsorption on $Co_2[Fe(CN)_6]/Fe_3O_4$

After the reaction reached the balance condition, there were a corresponding change in the material of Cs^+ and Co^{2+} in the reaction. The absorbed mili-equivalent of Co^{2+} was created in solution 0.2 m_{eq}/mL. As we can see, there changed the appearance of Fe ion because it was diluted by the surface of the absorbent. The amount of Co^{2+} appeared in the solution corresponding to the losing of Cs^+ after the reaction while there weren't any Co^{2+} in the solution before the reaction.

4. Conclusions

The achievement of this study is successfully synthesize the $Co_2[Fe(CN)_6]/Fe_3O_4$ material in nano size which can effectively absorb Cs^+ ion. $Co_2[Fe(CN)_6]$ constitutes 20.56 % of the weight of $Co_2[Fe(CN)_6]/Fe_3O_4$, which is paramagnetic material and easily separated from the solution by using magnet. The Cs+ adsorption process of this material based on the ion structure exchange. The ion exchange process of this material occurred effectively at pH = 4.0. The maximum absorption capacity of the material at pH = 4.0 for ion Cs^+ was 0.40 meq/g, and around 98% of initial Cs^+ concentration was removed.

ACKNOWLEDGMENTS

The authors wish to thank the Nuclear Engineering Department, Dalat University (VietNam) who sponsored the equipment for this research.

REFERENCES

[1]. E. H. Borai, R. Harjula, L. Malinen, A Paajanen, J Hazard Mater, pages 416-422, 2009

[2]. T. A. Todd, V. N. Romanovskiy, T.A. & Romanovskiy, V.N. Radiochemistry, Pages 364-367, 2005

[3]. P. A. Hass, Separation Science and Technology, Pages 2479-2506, 1993

[4]. H. Mimura, J. Lehto, R. Harjula, Journal of Nuclear Science and Technology, pages 1343-1350, 1997

[5]. C. Dwivedi, S. K. Pathak, M. Kumar, S. C. Tripathi, P. N. Bajai, RSC Advances, pages 8286-8290, 2013